

Role of Conserved Glycines in pH Gating of Kir1.1 (ROMK)

Henry Sackin,* Mikheil Nanazashvili,* Lawrence G. Palmer,[†] and Hui Li*

*Department of Physiology and Biophysics, The Chicago Medical School, North Chicago, Illinois 60064; and [†]Department of Physiology and Biophysics, Weill Medical College of Cornell University, New York, New York 10021

ABSTRACT Gating of inward rectifier Kir1.1 potassium channels by internal pH is believed to occur when large hydrophobic leucines, on each of the four subunits, obstruct the permeation path at the cytoplasmic end of the inner transmembrane helices (TM2). In this study, we examined whether closure of the channel at this point involves bending of the inner helix at one or both of two highly conserved glycine residues (corresponding to G134 and G143 in KirBac1.1) that have been proposed as putative “gating hinges” for potassium channels. Replacement of these conserved inner helical glycines by less flexible alanines did not abolish gating but shifted the apparent pKa from 6.6 ± 0.01 (wild-type) to 7.1 ± 0.01 for G157A-Kir1.1b, and to 7.3 ± 0.01 for G148A-Kir1.1b. When both glycines were mutated the effect was additive, shifting the pKa by 1.2 pH units to 7.8 ± 0.04 for the double mutant: G157A+G148A. At this pKa, the double mutant would remain completely closed under physiological conditions. In contrast, when the glycine at G148 was replaced by a proline, the pKa was shifted in the opposite direction from 6.6 ± 0.01 (wild-type) to 5.7 ± 0.01 for G148P. Although conserved glycines at G148 and G157 made it significantly easier to open the channel, they were not an absolute requirement for pH gating in Kir1.1. In addition, none of the glycine mutants produced more than small changes in either the cell-attached or excised single-channel kinetics which, in this channel, argues against changes in the selectivity filter. The putative pH sensor at K61-Kir1.1b, (equivalent to K80-Kir1.1a) was also examined. Mutation of this lysine to an untitratable methionine did not abolish pH gating, but shifted the pKa into an acid range from 6.6 ± 0.01 to 5.4 ± 0.04 , similar to pH gating in Kir2.1. Hence K61-Kir1.1b cannot function as the exclusive pH sensor for the channel, although it may act as one of multiple pH sensors, or as a link between a cytoplasmic sensor and the channel gate. K61-Kir1.1b also interacted differently with the two glycine mutations. Gating of the double mutant: K61M+G148A was indistinguishable from K61M alone, whereas gating of K61M+G157A was midway between the alkaline pKa of G157A and the acid pKa of K61M. Finally, closure of ROMK, G148A, G157A, and K61M all required the same L160-Kir1.1b residue at the cytoplasmic end of the inner transmembrane helix. Hence in wild-type and mutant channels, closure occurs by steric occlusion of the permeation path by four leucine side chains (L160-Kir1.1b) at the helix bundle crossing. This is facilitated by the conserved glycines on TM2, but pH gating in Kir1.1 does not absolutely require glycine hinges in this region.

INTRODUCTION

Despite advances in the structural biology of K channels (1–4), and inward rectifiers in particular (5,6), the mechanism of K channel gating is still unresolved. In the Kir1.1 inward rectifier family there is evidence that the pH gate appears to be centered at a convergence of four hydrophobic residues at the cytoplasmic apex of the inner transmembrane (TM) helices (5–7). Conceivably, a gate located at this position could open and close by a hinging mechanism (5,8–10) or by a rotation of adjacent subunits, or both (6).

Two glycine residues on the inner (M2) transmembrane helices are highly conserved throughout the inward rectifier family (Fig. 1, sequence alignment). The more N-terminal of these glycines (G148-Kir1.1b) has been implicated as a hinge point for bending of the inner helix during opening and closing of inward rectifiers (6,10), as well as in KcsA and MthK (9) and *Shaker* (8).

A second conserved glycine close to the cytoplasmic end of the inner transmembrane helix (G157-Kir1.1b) has also

been implicated as a possible hinge point for inward rectifier gating (6,10). In the *Shaker* Kv channel, the residue homologous to G157-Kir1.1b is contained within the amino acid sequence: Pro-Val-Pro, which may function as the physical gate of the *Shaker* channel (1,11–13).

In the present study, we examine whether these conserved glycines: G148 and G157 are involved in the pH gating mechanism of the renal inward rectifier, Kir1.1b (ROMK). Our results indicate that pH gating can still occur when one or both glycines are replaced by less flexible alanines. However, this shifts the apparent pKa into the alkaline range, making these mutant channels much harder to open relative to wild-type ROMK.

METHODS

Mutant construction and expression of channels

Point mutations in Kir1.1b (ROMK2; EMBL/GenBank/DBJ accession No. L29403) were engineered with a PCR QuickChange mutagenesis kit (Stratagene, La Jolla, CA), using primers synthesized by Integrated Data Technologies (Coralville, IA). Nucleotide sequences were checked on an Applied Biosystems (Foster City, CA) 3100 DNA sequencing machine at the University of Chicago Cancer Research Center.

Plasmids were linearized with *NotI* restriction enzyme and transcribed in vitro with T7 RNA polymerase in the presence of the GpppG cap using

Submitted October 25, 2005, and accepted for publication February 2, 2006.

Address reprint requests to Dr. Henry Sackin, Dept. of Physiology and Biophysics, The Chicago Medical School, Rosalind Franklin University of Medicine and Science, 3333 Green Bay Rd., North Chicago, IL 60064. Tel.: 847-578-8329; Fax: 847-578-3265; E-mail: henry.sackin@rosalindfranklin.edu.

© 2006 by the Biophysical Society

0006-3495/06/05/3582/08 \$2.00

doi: 10.1529/biophysj.105.076653

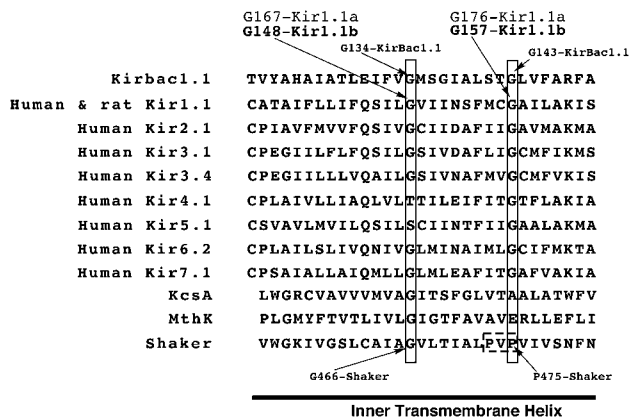


FIGURE 1 Two glycines on the inner transmembrane helices are highly conserved throughout the inward rectifier family (rectangles). One of these is also conserved in *Shaker*, and the other is part of a *Shaker* P-X-P motif that is highly conserved in voltage-gated K channels (dashed box).

mMESSAGE mMACHINE kit (Ambion, Austin, TX). Synthetic cRNA was dissolved in water and stored at -70°C before use. Stage V-VI oocytes were obtained by partial ovariectomy of female *Xenopus laevis* (NASCO, Ft. Atkinson, WI), anesthetized with tricaine methanesulfonate (1.5 g/L, adjusted to pH 7.0). Oocytes were defolliculated by incubation (on a Vari-Mix rocker) in Ca-free modified Barth's solution (82.5 mM NaCl, 2 mM KCl, 1 mM MgCl_2 , and 5 mM HEPES, adjusted to pH 7.5 with NaOH) containing 2 mg/ml collagenase type IA (Sigma Chemical, St. Louis, MO) for 90 min, and (if necessary) another 90 min in a fresh enzyme solution at 23°C . Oocytes were injected with 0.5 to 1 ng of cRNA and incubated at 19°C in $2\times$ diluted Leibovitz medium (Life Technologies, Grand Island, NY) for 1 to 3 days before measurements were made.

Whole-cell experiments

Whole-cell currents and conductances were measured in intact oocytes using a two-electrode voltage clamp (TEVC) (model CA-1, Dagan, Minneapolis, MN) with 16 command pulses of 30 ms duration between -200 mV and $+100$ mV, centered around the resting potential. Oocytes expressing ROMK or mutants of ROMK were bathed in permeant acetate buffers to control their internal pH as previously described (14–16). The composition of the bath for the whole-cell experiments was: 50 mM KCl, 50 mM K acetate, 1 M MgCl_2 , 2 mM CaCl_2 , 5 mM HEPES, and 1 mM SITS (4-acetamido-4-isothiocyanostilbene-2,2'-disulfonic acid). SITS was used to minimize small endogenous chloride currents; however batches of oocytes exhibiting chloride currents larger than $1\ \mu\text{A}$ were discarded, as were oocytes that did not exhibit at least a 40-mV shift in membrane potential for a 10-fold change in external [K].

Use of permeant buffers to control internal oocyte pH has the disadvantage that control of internal pH requires external pH to be changed as well. Although wild-type ROMK exhibits no significant external pH dependence at the voltages used, some of the mutants did have a measurable external pH dependence. Consequently, all of the two electrode voltage clamp currents were corrected for external pH by first running complete pH cycles with impermeant buffers, in which only outside pH was changed. The same oocytes were then subjected to both internal and external pH changes using permeant acetate buffers. In this way, each oocyte served as its own control, assuming that external and internal pH responses are independent processes.

Control of oocyte pH with permeant buffers required calibration of internal pH as a function of the applied outside pH. A previous calibration for ROMK expressing oocytes resulted in the following linear relationship

between external (o) and internal (i) pH: $\text{pH}_i = 0.595 \times \text{pH}_o + 2.4$ (16). This calibration was verified in the first section of the Results, by comparing pH titration curves determined with either permeant buffers or excised (inside-out) patches.

Because the mutant channels had somewhat different degrees of inward rectification, pH titration curves were constructed from inward conductances and were normalized to the maximum conductance to compensate for different expression efficiencies between channel types.

All oocytes were preincubated in 100 mM K solutions (50 mM Cl + 50 mM acetate) for 45 min at pH 7.8 to standardize their prior history of K exposure.

Patch-clamp experiments

Cell-attached recordings that were stable for 30 min or longer were used to compare the single-channel properties of the putative glycine hinge mutants to wild-type Kir1.1. In cell-attached mode, internal oocyte pH was controlled with permeant acetate buffers, similar to the two-electrode voltage clamp experiments described above. In addition to acetate, the bath contained 100 mM K and 2 mM Ca and was buffered with 5 mM HEPES to a pH of 7.8. The pipette solution also contained 100 mM K, but no divalents. Osmolarities were adjusted to 205 ± 5 mOsmol/L with NaCl.

Determinations of channel activity were conducted exclusively on inward currents because these give clear, well-defined transitions between open and closed states. The high open probability of Kir1.1 channels made it relatively easy to determine the number of active channels in a given patch. Only patches containing a single channel were used for kinetic analyses.

Excised inside-out patch recordings were used to examine the effect of cytoplasmic-side pH on channel activity in both wild-type and mutant channels. Rundown of channel activity in excised patches was prevented by using FVVP solutions in the bath (17). The composition of FVVP was: 100 mM K, no divalents, 5 mM EDTA, 4 mM NaFluoride, 3 mM Na orthovanadate, and 10 mM NaPyrophosphate, buffered with 5 mM HEPES to the desired pH.

To facilitate comparison between excised patches and intact oocytes, we counted the number of active channels in each excised patch during sequential exposure to different pH's. Because this method unambiguously determines inward rectifier currents, there was no need for leak subtraction (7). Both excised patch activity and inward whole-cell conductance were separately normalized and plotted as functions of internal pH.

Patch-clamp pipettes were pulled from 75 mm borosilicate glass (No. G85165T-3, Warner Instruments, Hamden, CT) using a two-stage process (L/M-3P-A puller) and coated with Sylgard (Dow Corning, Midland, MI). In all patch-clamp experiments, the oocyte vitelline membrane was removed with forceps following a brief exposure to hypertonic (450 mosmol/L) solution.

Pipette resistances ranged from 5 to 10 M Ω . Currents were recorded with a Dagan 8900 patch-clamp amplifier and stored, unfiltered, on videotape using Instrutech (Port Washington, NY) hardware (VR-10B and ITC-16). Single-channel events were sampled at 5 kHz and analyzed off-line using Bruyton (Seattle, WA) software (Acquire 4.0.10 and Tac/TacFit 4.1.5). The pH titration curves were fitted to a sigmoidal dose-response curve using Prism 4.0c software. All statistical comparisons were conducted using Statview 5.05 software (Cary, NC).

Experiments were performed at room temperature ($21 \pm 2^{\circ}\text{C}$) on Kir1.1b (ROMK2) or mutants of ROMK2 expressed in *Xenopus* oocytes.

RESULTS

Intact oocytes and excised patches

Previous experiments have indicated that ROMK (Kir1.1) is strongly gated by internal pH in both intact oocytes and excised patches (7,15,18–22). In these experiments, we used

the two electrode voltage clamp to re-measure the pH sensitivity of ROMK in oocytes whose internal pH was modulated with permeant acetate buffers (Fig. 2, *solid blue curve*). Internal pH was calculated from the calibration given in the Methods section. This curve is in good agreement with previous ROMK pH titrations determined either in cut-open oocytes (22) or with other permeant buffer systems (15).

Nonetheless, we were concerned about the effectiveness of permeant buffers to control internal oocyte pH. Consequently, we compared intact oocyte pH titrations with excised (inside-out) patch titrations. The results for excised ROMK are given by the dashed curve (*open red triangles*) of Fig. 2. This curve is indistinguishable from the two-electrode voltage clamp pH titration curve for ROMK (Fig. 2, *solid line, inverted blue triangles*).

To investigate whether acetate buffers were effective at controlling internal pH over a wide range, we compared excised and intact pH titration curves for a mutant (G148A) having a more alkaline pKa than ROMK. Fig. 3 shows inside-out patch recordings of both ROMK and this mutant (G148A-Kir1.1b). Channel rundown was prevented by FVVP in the bath solution (see Methods). Both ROMK and G148A are characterized by high open probability and flickery closures, where the rapid kinetics of the channel reflect interactions between permeant K ions and the selectivity filter (23).

As shown in Fig. 3, decreasing cytoplasmic-side pH reduced channel activity for both ROMK and G148A. The time course of activity change is a function of the rate at which bath pH is changed (starting at the vertical arrow). Control recordings with excised patches at constant pH did not exhibit decreases in channel activity as long as FVVP

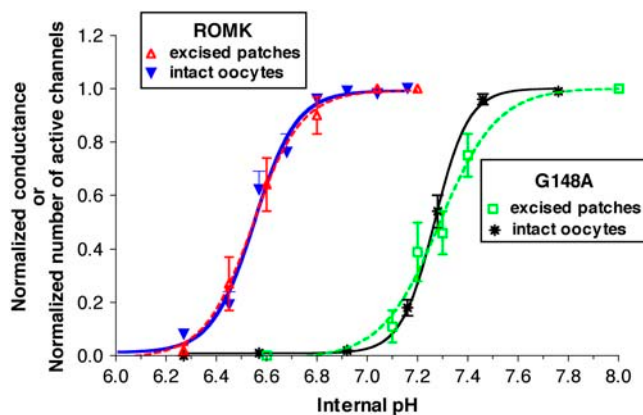


FIGURE 2 Comparison of excised and intact oocyte pH titrations for ROMK (Kir1.1b) and the G148A-Kir1.1b mutant. Pipette and bath solutions contained 100 mM K as described in the Methods section. Whole-cell ROMK (*inverted solid blue triangles*, pKa = 6.6 ± 0.02 , slope = 5.1, $n = 4$ oocytes). Excised patch ROMK (*open red triangles*, pKa = 6.6 ± 0.01 , slope = 4.5, $n = 6$ oocytes). Whole-cell G148A (*black stars*, pKa = 7.3 ± 0.01 , slope = 6.5, $n = 5$ oocytes). Excised patch G148A (*open green squares*, pKa = 7.3 ± 0.03 , slope = 3.8, $n = 5$ oocytes).

bath solutions were used. At bath perfusion rates of 4 ml/min, ~ 20 s were required for a 95% change in bath (cytoplasmic side) solution. During this period the exact pH at the internal face of the patch is between the two steady-state pH values given.

The single-channel kinetics of wild-type Kir1.1 and the two glycine mutants (G148A-Kir1.1b, G157A-Kir1.1b) are summarized in Table 1. All the kinetic data were obtained on patches containing only a single channel in either the cell attached or excised modes. The kinetics of the two glycine mutants were similar to the kinetics of native ROMK, suggesting that neither the G148A nor the G157A mutation produced major changes in tertiary structure, and did not substantially alter the region around the selectivity filter. However, G148A did have somewhat shorter open times and lower open probabilities than ROMK, whereas G157A had both shorter open and shorter closed times, but no difference in open probabilities (Table 1).

The excised-patch pH titration curve for G148A (Fig. 2, *open squares, dashed green line*) was constructed from experiments similar to those of Fig. 3, where the normalized number of active channels in each excised patch was plotted as a function of cytoplasmic side (bath) pH, using each patch as its own control. As shown in the figure, there was no significant difference between the G148A pH titrations obtained with either excised patches or intact oocytes and permeant buffers (Fig. 2, *asterisks, solid black line*). Both of the G148A curves are alkaline shifted relative to ROMK. These results confirm that the permeant acetate system can effectively control internal oocyte pH between pH 6 and 8, consistent with our previous calibration: $pH_i = .595 \times pH_o + 2.4$ (16). Consequently, most of the remaining titrations in this study were determined using the TEVC on intact oocytes, which allowed construction of reliable titration curves, even for mutants having a low expression efficiency.

Role of conserved glycines in pH gating

Conserved glycines in the inner transmembrane helix of both ligand and voltage-gated channels have been implicated as possible hinges in K channel gating (6,8,9,24). Mutating either or both of these glycines did not abolish pH gating, but did alter it significantly, indicating that G148A and G157A are probably both important in the Kir1.1b gating mechanism.

Fig. 4 depicts the intact oocyte pH titration curves for mutations at the two putative glycine hinges of Kir1.1 (*rectangles*, Fig. 1). Replacing the first glycine by a less flexible alanine residue shifted the pKa for gating by 0.7 pH units from 6.6 ± 0.01 (ROMK) to 7.3 ± 0.01 (G148A-Kir1.1b). Replacing the second conserved glycine (G157) by alanine shifted the apparent pKa by 0.6 pH units to 7.13 ± 0.01 (G157A-Kir1.1b). The combined effect of mutating both glycines to alanine was additive, altering the apparent pKa by 1.2 pH units from 6.6 (ROMK) to 7.8 ± 0.04 for

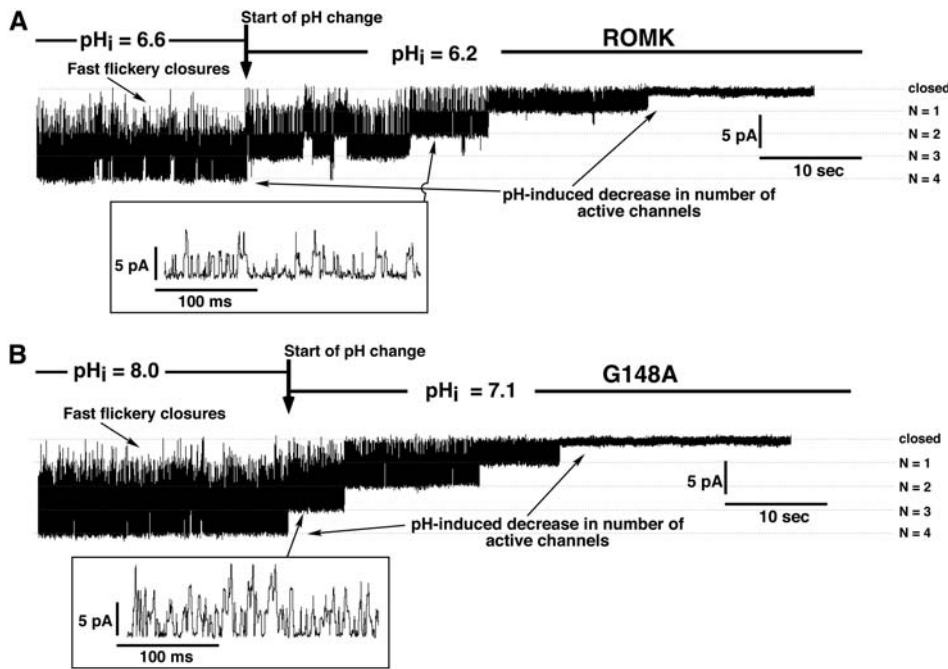


FIGURE 3 ROMK and G148A-Kir1.1b currents recorded from excised (inside-out) patches. Pipette solution: 100 mM K, 0 Mg, 2 Ca. Bath solution: FVVP solution with 100 mM K (see Methods). Pipette holding potential (relative to bath) = 100 mV. Records filtered at 800 Hz. Insets show currents at expanded timescale. At a bath flow rate = 4 ml/min; ~20 s were required for a 95% solution exchange. (A) Progressive decrease in the number of active ROMK channels as bath (cytoplasmic side) pH was reduced from 6.6 to 6.2. Current amplitude = 3.4 pA. (B) Progressive decrease in the number of active G148A-Kir1.1b channels as bath (cytoplasmic side) pH was reduced from 8 to 7.1. Current amplitude = 3.5 pA.

(G148A+G157A). This suggests that the two mutations stabilize the closed state relative to the open state through independent mechanisms.

We also introduced a proline at the G148 locus, which should produce a rigid kink in the helix at this point. Results for this mutant (Fig. 4, *green line*) indicate that G148P shifted the apparent pKa of the channel from $6.6 \pm .01$ (ROMK) to 5.7 ± 0.1 , thereby allowing the channel to remain open at significantly lower internal pH. This mutation also reduced the steepness of the pH titration curve.

The outer helix lysine (K61-Kir1.1b) and pH gating

A lysine (K61-Kir1.1b) near the junction between the outer helix and the slide helix has been implicated as a critical residue for internal pH sensing (14,15,20,22). Mutation of this positively charged lysine to methionine (a residue with a nonpolar side chain) did not abolish the pH sensitivity of the channel but merely shifted it into the acid range (Fig. 5,

green line), similar to what is seen with the Kir 2.1 strong inward rectifier (25). In 100 mM K solutions, the K61M-Kir1.1b mutant had a pKa of 5.4 ± 0.05 and a Hill slope of 1.6 ± 0.3 , compared to wild-type Kir1.1, which had a pKa of 6.6 ± 0.02 and a Hill slope of between 4 and 5 (Fig. 5, *blue line*).

Combining the K61M mutation with the L160G-Kir1.1b mutation effectively abolished pH gating, even in the extreme acid range (Fig. 5, *dashed purple line*). This implies that the pH gating of K61M still relies on the hydrophobic leucines at the putative L160 pH gate to block the permeation path in the closed state (7).

If the K61M mutation merely shifts the pKa but leaves the pH-gating mechanism unchanged, then the shift in pKa produced by G157A (relative to ROMK) should be approximately the same as the shift in pKa of G157A-K61M (relative to K61M). In fact, the ΔpKa between G157A-K61M and K61M was 1.1 ± 0.04 vs. 0.6 ± 0.02 for the difference between G157A and ROMK (Fig. 5, *horizontal*

TABLE 1 Single-channel parameters of ROMK and glycine mutants

	ROMK(Kir1.1b)	G157A-Kir1.1b	G148A-Kir1.1b	G148A-Kir1.1b
Mode	Cell-attached	Cell-attached	Cell-attached	Excised
Open probability	$0.91 \pm 0.01(5)$	$0.91 \pm 0.02(6)$	$0.77 \pm 0.03^*(7)$	$0.75 \pm 0.04^*(5)$
Open time (ms)	$20.6 \pm 1(5)$	$12.2 \pm 2(6)$	$6.7 \pm 0.7^*(7)$	$6.5 \pm 1^*(5)$
Closed time (ms)	$1.6 \pm 0.1(5)$	$0.8 \pm 0.1^*(6)$	$1.7 \pm 0.1(7)$	$1.9 \pm 0.1(5)$
Conductance (pS)	$47.0 \pm 2(6)$	$47.3 \pm 3(3)$	$48.6 \pm 1(7)$	$45.6 \pm 2(5)$

Data were obtained on single-channel, cell-attached, or excised (inside-out) patches with 100 mM K in the pipette and bath. The patch pipette contained no divalents for either cell-attached or excised patches. The presence of divalents in the patch pipette reduced single-channel conductance by ~30%. Holding potential was adjusted to obtain an inward current of ~5 pA. Kinetic parameters were determined for patches having only a single channel. Number of oocytes is given in parentheses.

*Denotes significant difference from ROMK ($P < 0.005$).

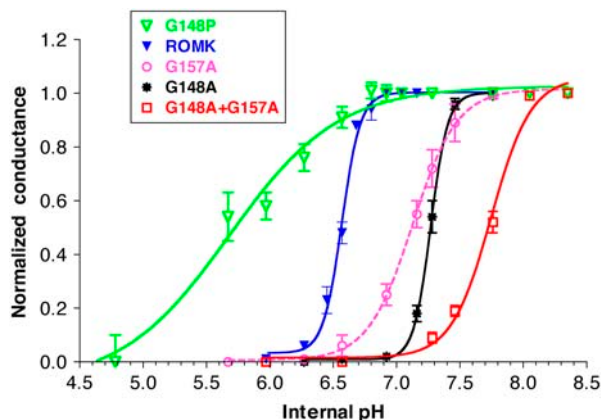


FIGURE 4 Mutation of the putative glycine hinges alters pH gating in Kir1.1b; pH titration curves on intact oocytes whose internal pH was controlled with permeant acetate buffers. Bath contained 100 mM K. See Methods for internal pH calibration and explanation of external pH correction. ROMK2 (*inverted solid blue triangles*, $pK_a = 6.6 \pm 0.02$, slope = 5.1, $n = 4$ oocytes). G148P (*open inverted green triangles*, $pK_a = 5.7 \pm 0.1$, slope = 1.0, $n = 5$ oocytes). G157A (*open magenta circles*, $pK_a = 7.1 \pm 0.01$, slope = 2.5, $n = 7$ oocytes). G148A (*black asterisks*, $pK_a = 7.3 \pm 0.01$, slope = 6.5, $n = 5$ oocytes). G148A+G157A (*open red squares*, $pK_a = 7.8 \pm .04$, slope = 2.8, $n = 7$ oocytes).

dashed arrows). This difference in ΔpK_a 's implies that the K61M mutation alters a fundamental aspect of the pH gating mechanism.

In the case of the double mutant, G148A-K61M, the K61M mutation clearly dominated over the effect of G148A (Fig. 6). The ΔpK_a between G148A-K61M and K61M was 0.08 ± 0.05 vs. 0.72 ± 0.02 for the difference between

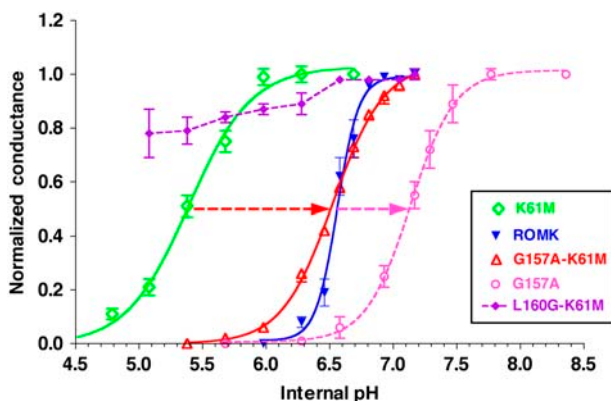


FIGURE 5 Effect of the K61M mutation and the combined K61M-glycine hinge mutations on pH gating in Kir1.1b, measured in intact oocytes whose internal pH was controlled with permeant acetate buffers. Bath contained 100 mM K. See Methods for internal pH calibration and explanation of external pH correction. ROMK2 (*inverted solid blue triangles*, $pK_a = 6.6 \pm 0.02$, slope = 5.1, $n = 4$ oocytes). L160G-K61M (*solid purple diamonds*, $n = 8$ oocytes). K61M (*open green diamonds*, $pK_a = 5.4 \pm 0.04$, slope = 1.8, $n = 3$ oocytes). G157A-K61M (*open red triangles*, $pK_a = 6.5 \pm 0.01$, slope = 2.2, $n = 4$ oocytes). G157A (*open magenta circles*, $pK_a = 7.1 \pm 0.01$, slope = 2.5, $n = 7$ oocytes). Dashed arrows denote the shifts in pK_a produced by the G157A mutation.

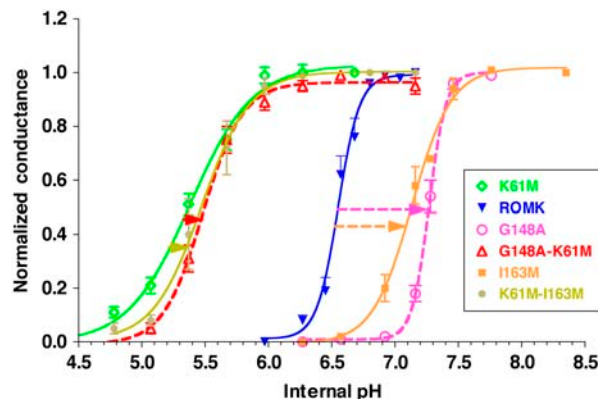


FIGURE 6 Combination of K61M and the glycine hinge G148A mutation on pH gating in Kir1.1b, measured in intact oocytes whose internal pH was controlled with permeant acetate buffers. Bath contained 100 mM K. See Methods for internal pH calibration and explanation of external pH correction. ROMK2 (*inverted solid blue triangles*, $pK_a = 6.6 \pm 0.02$, slope = 5.1, $n = 4$ oocytes). K61M (*open green diamonds*, $pK_a = 5.4 \pm 0.04$, slope = 1.8, $n = 3$ oocytes). G148A-K61M (*open red triangles*, $pK_a = 5.5 \pm 0.02$, slope = 2.8, $n = 7$ oocytes). I163M-K61M (*solid circles*, $pK_a = 5.5 \pm .02$, slope = 2.3, $n = 4$ oocytes). I163M (*solid squares*, $pK_a = 7.1 \pm .02$, slope = 2.8, $n = 4$ oocytes). G148A (*open magenta circles*, $pK_a = 7.3 \pm 0.01$, slope = 6.5, $n = 5$ oocytes). Dashed arrows denote the shifts in pK_a produced by the G148A mutation.

G148A and ROMK (Fig. 6, *horizontal arrows*). This effect of K61M on G148A was not unique. Another mutant (I163M), whose pK_a was also in the alkaline range, showed a similar interaction with K61M. In this case, the ΔpK_a between I163M-K61M and K61M was 0.09 ± 0.05 vs. 0.6 ± 0.03 for the difference between I163M and ROMK (Fig. 6). Hence, the K61 residue appears essential for normal pH gating, even though it is not the exclusive pH sensor for the channel.

Effect of L160G on G148A and G157A

Because the conserved glycines at G148 and G157 appear to play an important role in pH gating of Kir1.1, it makes sense to ask how these putative glycine hinges interact with the leucine residue L160-Kir1.1b, which is believed to occlude the permeation path of Kir1.1 in the closed state (6,7). If pH gating of Kir1.1 involves a hinged movement of the inner helix at G148A and/or G157A, mutating the leucine at L160 should disrupt gating not only in wild-type but also in the alkaline shifted mutants, G148A and G157A.

As indicated in Fig. 7, G148A-L160G and G157A-L160G were as insensitive to internal pH as the single L160G mutant (7). Replacement of Leu-160 by the sterically smaller glycine prevented closure of both wild-type and glycine mutants. This suggests that ROMK, G148A, and G157A all utilize the same hydrophobic leucines (L160-Kir1.1b) to close the permeation path at the cytoplasmic end of the inner transmembrane helix.

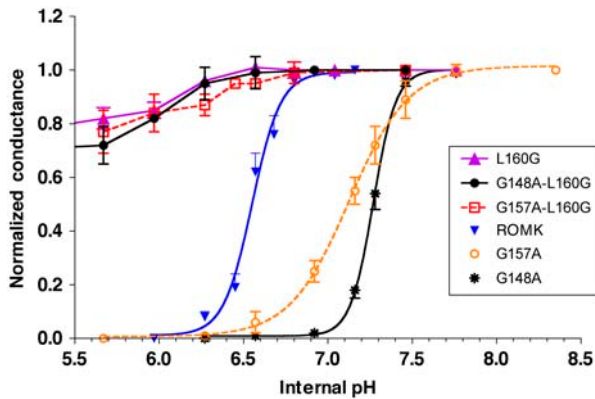


FIGURE 7 Effect of the L160G mutation on the putative glycine hinge mutants, measured in intact oocytes whose internal pH was controlled with permeant acetate buffers. Bath contained 100 mM K. See Methods for internal pH calibration and explanation of external pH correction. L160G-Kir1.1b (solid purple triangles, $n = 4$ oocytes). G148A-L160G (solid black circles, $n = 4$ oocytes). G157A-L160G (open red squares, dashed line, $n = 5$ oocytes). ROMK2 (inverted blue triangles, $pK_a = 6.6 \pm 0.02$, slope = 5.1, $n = 4$ oocytes). G157A (open orange circles, $pK_a = 7.1 \pm 0.01$, slope = 2.5, $n = 7$ oocytes). G148A (black asterisks, $pK_a = 7.3 \pm 0.01$, slope = 6.5, $n = 5$ oocytes).

DISCUSSION

Role of conserved glycines in gating

Comparison of the closed-state crystal structure of KirBac1.1 (6) with the presumed open-state structure of KirBac3.1 (5) implied that gating of Kir channels occurs when hydrophobic residues near the cytoplasmic end of the inner transmembrane helices occlude the permeation path (5–7,10). The mechanism for this closure is thought to involve bending of the inner transmembrane helix at one or more putative glycine hinges, G134 and G143 in KirBac1.1, which are homologous to G148 and G157 in Kir1.1b (1,5,6,8,9,11–13, 24,26). However, x-ray diffraction data may or may not depict actual physiological states. Hence, we elected to test the applicability of this glycine-hinge hypothesis to pH gating in the mammalian renal inward rectifier, ROMK (Kir1.1).

Kir1.1 is sensitive to internal pH, with acidification blocking the channel and preventing K efflux across the apical membranes of cortical collecting tubule and thick ascending limb of Henle (14,15,18,21,27). This sensitivity to internal pH was confirmed in this study, using both excised patches and whole-cell currents from ROMK-expressing oocytes.

Previous studies have highlighted the importance of conserved inner-helix glycines in K channel gating (1,5,6,8–10). In *Shaker*, the single point mutation at G466A (homologous to G148A-Kir1.1b) abolished channel current. However, this may not be entirely due to changes in flexibility at this point in the helix, because G466A also had impaired glycosylation and possibly improper folding in the endoplasmic reticulum (8,24). Less drastic effects of Gly to Ala mutations were reported for the G311A mutation (also

homologous to G148A-Kir1.1b) in BK channels (8) and for the G219A mutation in bacterial Na channels (28). The effects of these mutations were similar to the shifts in apparent pK_a produced by the Kir1.1b glycine mutations, reinforcing the notion that inner-helix glycines are important, but not absolutely essential for Kir gating.

In our studies on Kir1.1, mutation of both conserved inner helix glycines to alanines did not abolish pH gating but alkaline-shifted the apparent pK_a in an additive fashion. Namely, the combined effect of G148A and G157A (= 1.2 pH units) was close to the sum of the individual mutations: G148A (= 0.7 pH units) and G157A (= 0.6 pH units). This suggested that both glycines contribute independently to the gating process.

The failure of either G148A or G157A to completely abolish gating in Kir1.1b clearly shows that gating does not absolutely require the presence of glycine hinges at either of these positions. One possibility is that the alanines used to replace the conserved glycines allow sufficient angular movement of the inner helix so that the mutants still gate, but at a higher pK_a . It is also possible that a hinge motion is not required for gating. Electron paramagnetic resonance studies of KcsA gating transitions suggest that a twisting and scissor-like movement of the inner transmembrane helices may be predominant steps for opening this channel. In fact, the region near residues 107, 108 on KcsA (corresponding to the G157 locus in Kir1.1b) was implicated as a pivot point for helix movement in KcsA (29,30). In this interpretation, the effect of the alanine for glycine substitution might be due to the larger alanine side chain introducing a steric hindrance to channel opening.

K61-Kir1.1b and pH gating

The finding of pH gating in the K61M mutant (Fig. 5) makes it unlikely that the K61-Kir1.1b (K80-Kir1.1a) residue functions as the exclusive pH sensor for the channel, as previously envisioned (31). However, K61 might still play a sensor role if its free solution pK_a of 10.5 were brought closer to 7 by interaction with either positive residues (19) or the membrane lipid environment, since K61 is now known to reside within the membrane, rather than in the cytoplasm (6).

Our data indicate that G148A and G157A react differently to the K61M mutation. The double mutation of G157A and K61M produced a titration curve midway between the individual curves for G157A and K61M and close to the value of the wild-type channel (Fig. 5). This suggests that G157A may be acting independently of the K61M mutation, with both mutations contributing oppositely (and about the same magnitude) to the final titration curve for G157A-K61M. This is in contrast to the double mutant G148A-K61M, which resulted in a titration curve that was indistinguishable from the K61M titration alone (5.5 ± 0.02 vs. 5.4 ± 0.05), and suggested a dominance of the K61M mutation over the G148A mutation (Fig. 6).

We also examined the effect of K61M on the I163M mutant, which was previously shown to gate in a more alkaline range than wild-type ROMK (7,32). The effect of the K61M mutation on I163M was similar to its effect on G148A, where the pKa of K61M-I163M was indistinguishable from that of K61M-G148A (Fig. 6).

These data imply that K61 is not absolutely essential for pH gating but could act as one of several pH sensors, in this case operating in the range above pH 6; whereas other pH sensor(s) might function at an internal pH below 6. Alternatively, K61 might be acting as an intermediary link between a cytoplasmic pH sensor and the putative physical gate at the bundle crossing of the inner helices (33).

Both G148A and G157A still rely on the putative gate at L160G

Regardless of how G148A and G157A alter pH gating, both of these glycine mutants still utilized leucine residues at L160-Kir1.1b to physically occlude the permeation path. Evidence for this comes from the finding that the double mutants, L160G-G148A and L160G-G157A, remained open at low internal pH, similar to the single point mutant, L160G-Kir1.1b.

Furthermore, the acid-shifted pH gating of the K61M mutant also depended on these same hydrophobic leucines at L160, since the double mutant L160G-K61M failed to close, even at extremely low pH (Fig. 5). Previous work had indicated that replacing the leucines at L160-Kir1.1b with residues having small or highly polar side chains allowed passage of hydrated K ions at low pH, when the gate would normally be closed (7). Hence, this study confirms a physiological gate at L160-Kir1.1b that is functionally separate from any bending of the inner helix, as well as from the pH sensor itself.

SUMMARY

We examined the role of two conserved, inner transmembrane helix glycines in pH gating of the Kir1.1 inward rectifier. Replacing one or both of these glycines by alanines did not abolish gating but shifted the apparent pKa of the channel into the alkaline range. The combined effect of removing both glycines alkalinized the pKa to a point where the channel would remain completely closed under physiological conditions. These results are consistent with structural (5,6) and electrophysiological (7) data, suggesting that pH gating occurs via steric occlusion of the permeation path by four leucine side chains at the helix bundle crossing, which is facilitated by conserved glycines on the inner transmembrane helix. However, pH gating in Kir1.1 does not absolutely require glycine hinges in this region.

The authors acknowledge the helpful discussions with Janice Robertson in the Department of Physiology and Biophysics at Weill Medical College of Cornell University.

This work was supported by National Institutes of Health grants DK46950 (H. Sackin) and DK27847 (L. G. Palmer).

REFERENCES

1. Long, S., E. Campbell, and R. MacKinnon. 2005. Crystal structure of a mammalian voltage-dependent *Shaker* family K channel. *Science*. 309:897–903.
2. Doyle, D. A., J. M. Cabral, R. A. Pfuetzner, A. Kuo, J. M. Gulbis, S. L. Cohen, B. T. Chait, and R. MacKinnon. 1998. The structure of the potassium channel: molecular basis of K⁺ conduction and selectivity. *Science*. 280:69–77.
3. Jiang, Y., A. Lee, J. Chen, V. Ruta, M. Cadene, B. Chait, and R. MacKinnon. 2003. X-ray structure of a voltage-dependent K channel. *Nature*. 423:33–41.
4. Zhou, Y., J. Morais-Cabral, A. Kaufman, and R. MacKinnon. 2001. Chemistry of ion coordination and hydration revealed by a K channel Fab complex at 2.0 Å resolution. *Nature*. 414:43–48.
5. Kuo, A., C. Domene, L. Johnson, D. Doyle, and C. Vénien-Bryan. 2005. Two different conformational states of the KirBac3.1 potassium channel revealed by electron crystallography. *Structure*. 13: 1–10.
6. Kuo, A., J. Gulbis, J. Antcliff, T. Rahman, E. Lowe, J. Zimmer, J. Cuthbertson, F. Ashcroft, T. Ezaki, and D. Doyle. 2003. Crystal structure of the potassium channel KirBac1.1 in the closed state. *Science*. 300:1922–1926.
7. Sackin, H., M. Nanazashvili, L. G. Palmer, M. Krambis, and D. E. Walters. 2005. Structural locus of the pH gate in the Kir1.1 inward rectifier channel. *Biophys. J.* 88:2597–2606.
8. Magidovich, E., and O. Yifrach. 2004. Conserved gating hinge in ligand- and voltage-dependent K channels. *Biochemistry*. 43:13242–13247.
9. Jiang, Y., A. Lee, J. Chen, M. Cadene, B. Chait, and R. MacKinnon. 2002. The open pore conformation of potassium channels. *Nature*. 417:523–526.
10. Domene, C., D. Doyle, and C. Vénien-Bryan. 2005. Modeling of an ion channel in its open conformation. *Biophys. J.* 89:L1–L3.
11. del Camino, D., M. Holmgren, Y. Liu, and G. Yellen. 2000. Blocker protection in the pore of a voltage-gated K channel and its structural implications. *Nature*. 403:321–325.
12. del Camino, D., and G. Yellen. 2001. Tight steric closure at the intracellular activation gate of a voltage-gated K channel. *Neuron*. 32:649–656.
13. Webster, S., D. del Camino, and G. Yellen. 2004. Intracellular gate opening in *Shaker* K channels defined by high-affinity metal bridges. *Nature*. 428:864–868.
14. Doi, T., B. Fakler, J. H. Schultz, U. Schulte, U. Brandle, S. Weidemann, H. P. Zenner, F. Lang, and J. P. Ruppersberg. 1996. Extracellular K⁺ and intracellular pH allosterically regulate renal Kir1.1 channels. *J. Biol. Chem.* 271:17261–17266.
15. Leipziger, J., G. MacGregor, G. Cooper, J. Xu, S. Hebert, and G. Giebisch. 2000. PKA site mutations of ROMK2 channels shift the pH dependence to more alkaline values. *Am. J. Physiol. Renal Physiol.* 279:F919–F926.
16. Choe, H., H. Zhou, L. G. Palmer, and H. Sackin. 1997. A conserved cytoplasmic region of ROMK modulates pH sensitivity, conductance, and gating. *Am. J. Physiol.* 273:F516–F529.
17. Leung, Y., W. Zeng, H. Liou, C. Solaro, and C. Huang. 2000. Phosphatidylinositol 4,5-bisphosphate and intracellular pH regulate the ROMK1 potassium channel via separate but interrelated mechanisms. *J. Biol. Chem.* 275:10182–10189.
18. Tsai, T. D., M. E. Shuck, D. P. Thompson, M. J. Bienkowski, and K. S. Lee. 1995. Intracellular H⁺ inhibits a cloned rat kidney outer medulla K⁺ channel expressed in *Xenopus* oocytes. *Am. J. Physiol.* 268:C1173–C1178.

19. Schulte, U., H. Hahn, M. Konrad, N. Jeck, C. Derst, K. Wild, S. Weidemann, J. Ruppersberg, B. Fakler, and J. Ludwig. 1999. pH gating of ROMK (Kir1.1) channels: control by an Arg-Lys-Arg triad disrupted in antenatal Bartter syndrome. *Proc. Natl. Acad. Sci. USA.* 96:15298–15303.
20. Schulte, U., S. Weidemann, J. Ludwig, J. Ruppersberg, and B. Fakler. 2001. K-dependent gating of Kir1.1 channels is linked to pH gating through a conformational change in the pore. *J. Physiol.* 534:49–58.
21. McNicholas, C. M., G. G. MacGregor, L. D. Islas, Y. Yang, S. C. Hebert, and G. Giebisch. 1998. pH-dependent modulation of the cloned renal K⁺ channel, ROMK. *Am. J. Physiol.* 275:F972–F981.
22. Sackin, H., A. Vasilyev, L. G. Palmer, and M. Krambis. 2003. Permeant cations and blockers modulate pH gating of ROMK channels. *Biophys. J.* 84:910–921.
23. Choe, H., H. Sackin, and L. G. Palmer. 1998. Permeation and gating of an inwardly rectifying potassium channel: evidence for a variable energy well. *J. Gen. Physiol.* 112:433–446.
24. Ding, S., L. Ingleby, C. Ahern, and R. Horn. 2005. Investigating the putative glycine hinge in *Shaker* potassium channel. *J. Gen. Physiol.* 126:213–226.
25. Sabirov, R., Y. Okada, and S. Oiki. 1997. Two-sided action of protons on an inward rectifier K channel (IRK1). *Pflugers Arch.* 433:428–434.
26. Jin, T., L. Peng, T. Mirshahi, T. Rohacs, K. Chan, R. Sanchez, and D. E. Logothetis. 2002. The $\beta\gamma$ subunits of G proteins gate a K channel by pivoted bending of a transmembrane segment. *Mol. Cell.* 10:469–481.
27. Sackin, H., S. Syn, L. G. Palmer, H. Choe, and E. Walters. 2001. Regulation of ROMK by extracellular cations. *Biophys. J.* 80: 683–697.
28. Zhao, Y., V. Yarov-Yarovoy, T. Scheuer, and W. A. Catterall. 2004. A gating hinge in Na channels: a molecular switch for electrical signaling. *Neuron.* 41:859–865.
29. Liu, Y. S., P. Sompompisut, and E. Perozo. 2001. Structure of the KcsA channel intracellular gate in the open state. *Nature.* 8:883–887.
30. Perozo, E., D. M. Cortes, and L. G. Cuello. 1999. Structural rearrangements underlying K-channel activation gating. *Science.* 285: 73–78.
31. Fakler, B., J. H. Schultz, J. Yang, U. Schulte, U. Brandle, H. P. Zenner, L. Y. Jan, and J. P. Ruppersberg. 1996. Identification of a titratable lysine residue that determines sensitivity of kidney potassium channels (ROMK) to intracellular pH. *EMBO J.* 15:4093–4099.
32. Dahlmann, A., M. Li, Z. Gao, D. McGarrigle, H. Sackin, and L. G. Palmer. 2004. Regulation of Kir channels by intracellular pH and extracellular K: mechanisms of coupling. *J. Gen. Physiol.* 123:441–454.
33. Leng, Q., G. G. MacGregor, K. Dong, G. Giebisch, and S. Hebert. 2006. Subunit-subunit interactions are critical for proton sensitivity of ROMK: evidence in support of an intermolecular gating mechanism. *Proc. Natl. Acad. Sci. USA.* 103:1982–1987.